J. Meas. Sci. Instrum., 2026, 17(1): 1-15. http://jmsi.publish.founderss.cn/
DOI: 10.62756/jmsi.1674-8042.2026001 jmsi@nuc.edu.cn

Microstructure-based terahertz sensing technology: from electromagnetic response enhancement to multi-scale detection

ZHANG Shu[1], NIU Wenyu[2], HAO Yafeng[2], MA Fupeng[2], ZHU Pu[2], WU Huijia[2], HUANG Yujie[2], LI Tengteng[2*], LIU Meihong[2*], LEI Cheng[2], LIANG Ting[2]

1. Tianjin Jinhang Institute of Technical Physics, Tianjin 300308, China;
2. State key Laboratory of Extreme Environment Optoelectronic Dynamic Measurement Technology and Instrument, North University of China, Taiyuan 030051, China

***Corresponding author:** LI Tengteng (litengteng@nuc.edu.cn); LIU Meihong (liumeihong@nuc.edu.cn)

Received: September 12, 2025 **Revised:** January 26, 2026 **Accepted:** January 30, 2026

Abstract: Terahertz (THz) waves exhibit distinctive properties, such as high transmittance, pronounced absorption, and minimal photon energy, enabling a wide range of applications in biomedical diagnosis, non-destructive testing, and quality/safety monitoring of food and agricultural products. Consequently, THz-based sensors have garnered increasing attention. However, the design of traditional coupling structures fails to effectively match the high-frequency oscillation of THz waves, resulting in low signal energy transmission efficiency and limiting the performance of THz sensors, while microstructure technology can offer a solution by achieving localized enhancement of the electromagnetic field energy through precise matching of sub-wavelength resonance units with the high-frequency oscillation of THz waves, which significantly improves the sensitivity of THz sensors. This review summarizes the basic principles and research status of various THz sensors based on different microstructures, such as split-ring resonators (SRRs), photonic crystals, waveguide resonators, and surface plasmon resonance. Notably, the rapid development of artificial intelligence, especially deep learning, is increasingly influencing THz sensing technologies with its strengths in signal processing, pattern recognition accuracy, and inverse design. Integrating deep learning with THz sensor design enhances feature extraction from complex signals, improves target identification, and enables intelligent optimization of microstructure parameters for high-performance sensor design and performance prediction. This interdisciplinary approach provides a new pathway to overcome traditional design limitations and advance THz sensor performance.

Key words: terahertz (THz); artificial microstructures; sensors; surface plasmon resonance; waveguides; photonic crystals; deep learning

0 Introduction

The frequency range of terahertz (THz) waves is typically defined between 0.1 THz and 10 THz, corresponding to wavelengths from 3 mm to 0.03 mm. The electromagnetic spectrum, positioned between microwaves and infrared waves[1-2], as depicted in Fig.1, is integral to the advancement of information technology and intelligent devices. As a foundational strategic resource, it underscores its essential role and core value in supporting digital applications across various sectors in modern society. Considerable research attention has recently converged on the THz frequency range in this scientific domain[3]. THz waves possess low photon energy[4], enabling THz detection technology to substantially mitigate damage to biomolecules compared to traditional methods. This advantage underscores the significant application potential of THz technology in biomedicine[5-6] and security inspection[7-8]. Furthermore, the electromagnetic radiation in the THz band exhibits excellent penetration characteristics[9], facilitating non-invasive detection within non-transparent packaging materials. THz waves are characterized by high spatial resolution, making them prevalent in wireless communication[10-12]. Moreover, the THz frequency band aligns with the resonance frequencies of numerous biological and chemical molecules, allowing these molecules to exhibit distinct resonance absorption and rich fingerprint spectra[13]. Elucidating the THz-wave interactions with biomolecules provides structural insights at the molecular level[14], facilitating precise detection capabilities[15-17].

The response capabilities of many natural materials in the THz band are limited[18-20]. To address this, researchers are investigating various microstructures[3]. Through precise engineering of the periodicity, geometric configuration, dimensional parameters, and positional organization of

these structures[21-22], it is possible to achieve electromagnetic responses unattainable with natural materials[23], such as negative refractive index, superlens effects[24], and near-perfect invisibility to electromagnetic waves[25]. These properties enable precise control and modulation of electromagnetic fields for specific functions[26]. THz artificial microstructure sensors, functioning as label-free and high-throughput optical sensing platforms, exploit the intrinsic merits of the THz spectrum, offering superior sensitivity and efficiency compared to other sensing technologies. This review examines the sensing mechanisms of THz sensors, summarizes key research findings, and explores the technological development of THz sensors based on micro- and nano-structures like split-ring resonator (SRR) structures[27], photonic crystals[28], waveguides[29], and surface plasmons[30-31]. It also discusses future trends in THz sensing technology.

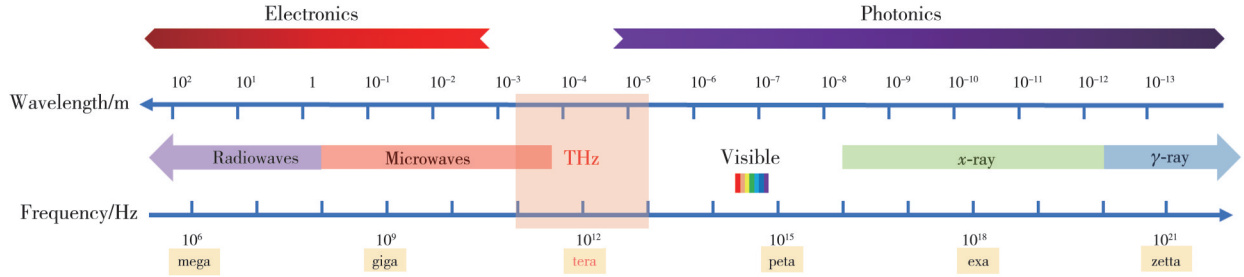

Fig. 1 Terahertz spectrum

1 Theoretical basis of THz microstructured sensors

1.1 Fundamental theories of metamaterials

Metamaterials are engineered sub-wavelength constructs featuring periodic or aperiodic unit structures. They are characterized by their permittivity (ε) and permeability (μ). The refractive index (n) is related to these parameters as follows:

$$n = \sqrt{\varepsilon\mu}\,. \tag{1}$$

Electromagnetic theory classifies media with positive ε and μ values as conventional right-handed media (RHM), capable of supporting electromagnetic wave propagation and commonly found in nature. Conversely, media exhibiting negative ε and μ values possess a negative refractive index and are termed left-handed media (LHM), which are artificially engineered metamaterials.

In metamaterial design, metal wires and SRRs are two key artificial structural units with distinct electromagnetic response mechanisms. Metal wires induce a dipole resonance effect, creating a coupling response with the electric field. Conversely, SRRs form an oscillatory response mechanism with magnetic field variations, based on the principles of a capacitance-inductance (LC) resonant circuit.

In examining the electromagnetic properties of elongated metallic conductors, researchers often utilize the Drude dispersion model to theoretically determine and calculate the structures' equivalent permittivity, as outlined by

$$\varepsilon_{\text{eff}}(\omega) = 1 - \frac{\omega_{\text{ep}}^2}{\omega^2 + \mathrm{j}\Gamma\omega}, \tag{2}$$

where Γ denotes the electromagnetic wave propagation loss term, while ω_{ep} is the effective plasma frequency of the metal wire. This frequency represents the maximum oscillation frequency attainable when the metal's free electrons collectively couple and resonate with an external electromagnetic field. ω_{ep} is derived from

$$\omega_{\text{ep}}^2 = \frac{2\pi c_0^2}{a^2 \ln(a/r)}, \tag{3}$$

where c_0 represents the reference value of the speed of light in a vacuum environment, a is the characteristic periodic length of the metal wire structure along the propagation direction, and r is the radial geometric dimension of the conductor cross-section. As can be seen from Eqs. (2) and (3), by systematically adjusting the geometric structure parameters of the metal wire, the characteristic plasma frequency ω_{ep} of the material can be effectively regulated, and ultimately, the directional control of its equivalent permittivity can be achieved.

The SRR can be regarded as a metallic open ring structure with a gap of a specific width. The conductive region can be modeled as an inductance, while the spatial separation constitutes a capacitive gap[32-33]. This structure can achieve local field enhancement[34] by utilizing the LC resonance mode, equivalently forming an LC oscillating circuit. Its resonance frequency is

$$\omega_{LC} = (LC)^{-1/2}. \tag{4}$$

Capacitance (C) and inductance (L) are key parameters in this context. The inductance L is primarily constrained by the structural unit's spatial scale, which dictates the metal

loop's spatial configuration and the inductor coil's geometric shape. In contrast, capacitance C is largely influenced by the dielectric properties of the surrounding medium and the spatial variation pattern of the induced electric field on the metasurface plane. The expression for C is given by

$$C=\frac{\varepsilon S_r}{4\pi kd}, \tag{5}$$

where S_r represents the effective cross-section, d denotes the distance between the capacitor plates, and ε corresponds to the dielectric constant, characterizing the medium's ability to store electrical energy. When the sample covers the metasurface sensor's structural unit, S_r and d remain constant, but the electromagnetic environment at the gap changes. This alters ε, which modifies the equivalent capacitance C, ultimately shifting the resonance frequency.

1.2 THz sensor sensing mechanism

THz sensors mainly achieve the identification of substance types based on the spectral characteristic differences of different substances in the THz frequency band. The key lies in designing various microstructures to interact with THz waves and converting the variation of the measured substance into detectable signals through multiple physical effects. Its sensing mechanisms include resonance effects, changes in refractive index, and variations in photonic band gaps. First, regarding the resonance effect, the microstructure can be designed as a specific resonant structure. When irradiated by THz waves, resonance occurs at a specific frequency. When the environment around the sensor changes, the resonance frequency will shift, or the amplitude of the resonance peak will change. These changes can be detected, thereby reflecting the information of the analyte. The refractive index, a fundamental optical parameter, significantly influences light wave propagation. Its real part governs phase modulation, while the imaginary part affects intensity attenuation. The anisotropic spatial distribution of the refractive index directly influences the polarization state of light waves. By designing specific microstructures, electromagnetic waves can be precisely manipulated. Subtle fluctuations in refractive index parameters can lead to considerable alterations in metamaterial electromagnetic behavior. Harnessing this effect, researchers have developed advanced THz refractive index sensing platforms for enhanced detection performance, where the presence of a substance can alter the local refractive index on the sensor surface. When THz waves interact with microstructures, Fluctuations in the refractive index parameter can significantly modify the propagation dynamics of electromagnetic waves, including phase delay and amplitude attenuation. These changes allow for the inference of the substance's properties, such as concentration and thickness. Similarly, photonic crystal sensors exploit shifts in the photonic bandgap for sensing. When the target substance enters the periodic structure of the photonic crystal, it modifies the dielectric constant distribution, shifting the bandgap position and thus affecting the transmission or reflection spectrum.

1.3 Main performance parameters

In the spectral shift sensing technology, the sensitivity S_f is one of the core performance parameters, which is the change in the resonant peak wavelength caused by a unit refractive index change. Sensitivity is usually measured in units of THz/RIU (THz per refractive index unit). When the content of the analyte remains constant, a higher S_f indicates a higher sensitivity of the device[35]. The mathematical definition of this parameter is the ratio of the resonance frequency offset Δf to the change in the analyte refractive index Δn, that is,

$$S_f=\frac{\Delta f}{\Delta n}. \tag{6}$$

In the performance evaluation dimension of optical resonant devices, the quality factor Q plays a central role as a key parameter, and its value directly reflects the energy retention characteristics of the resonant cavity. A higher Q value indicates a lower energy dissipation level in the corresponding resonant system, resulting in a more pronounced sharpening feature of the resonance spectral line, specifically manifested as a significant decrease in the full width at half maximum (FWHM). This parameter can be quantitatively calculated by the ratio of the resonant center frequency f_0 to the FWHM, that is,

$$Q=\frac{f_0}{FWHM}. \tag{7}$$

Meanwhile, the figure of merit (FOM) is also introduced as a quantitative evaluation index. Its conventional calculation method is to calculate the ratio of the sensitivity S_f to FWHM, that is,

$$FOM=\frac{S_f}{FWHM}. \tag{8}$$

The sensor performs optimally when it simultaneously exhibits high sensitivity and a high quality factor.

The core principle of a metamaterial-based THz sensor lies in the strategic design of the metamaterial's unit cell dimensions to be on the order of the THz wavelength. This

engineering ensures that its fundamental resonance frequency falls within the THz band. Upon illumination with a THz wave, the metamaterial undergoes a strong localized resonance, exhibiting extreme sensitivity to minute changes in the surrounding dielectric environment at its surface, thereby enabling highly sensitive detection of target analytes.

The sensitivity (S) of the sensor is directly proportional to the localized intensity of the electromagnetic field within the sensing region. A stronger field enhances the interaction with the analyte, leading to a more pronounced perturbation of the local dielectric environment. The structural design of the metamaterial, such as incorporating sharp corners or nanogaps, is paramount for enhancing this field localization.

The quality factor (Q-factor), originating from the resonance sharpness and the system's energy loss mechanisms, defines the spectral resolution. A high Q-factor necessitates minimal metallic and radiative losses in the metamaterial resonator. A sharp resonance peak facilitates the detection and resolution of minute frequency shifts. It is important to note that a design trade-off often exists: structures engineered for extremely strong field localization (high sensitivity) may exhibit increased radiative losses, potentially leading to a degradation of the Q-factor. Consequently, sensor design necessitates a careful optimization trade-off between achieving high sensitivity and maintaining a high Q-factor.

2 Research status of THz sensors based on different microstructures

2.1 SRR structure sensor

The SRR sensor, leveraging its unique magnetic resonance mechanism and powerful field localization capabilities, extends high-sensitivity detection to realms such as magnetic field response, the THz band, and chiral molecular analysis. Its high degree of design freedom and miniaturization potential make it a paramount candidate for the core of next-generation ultrasensitive, integrated, and multifunctional photonic sensing chips, demonstrating immense application prospects in biomedical diagnostics, environmental monitoring, food safety, and fundamental scientific research. The fundamental SRR architecture incorporates a planar metallic square ring with an intentionally designed gap of specified dimension on one of its sides. To enhance sensing performance, approaches like asymmetric SRRs, improved SRR designs, and multiple SRR resonant units have been developed.

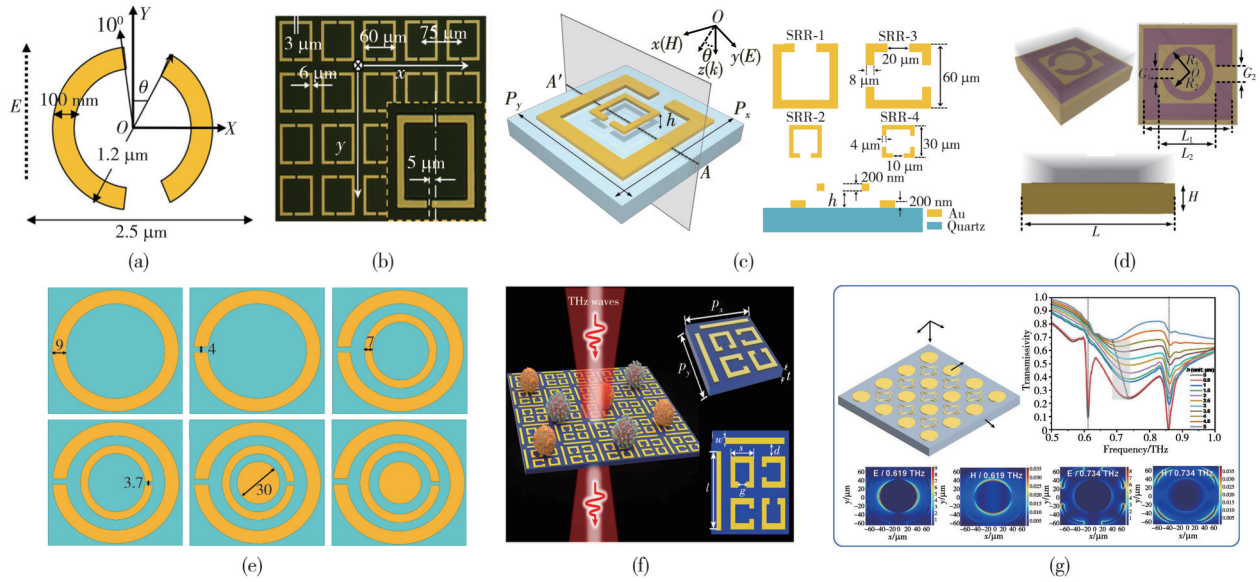

Fig. 2 Terahertz sensors with SRR structure. (a) Unit cell of a single A-SRR, (b) Asymmetric double-split SRR structure, (c) Schematic drawing of TTM, (d) Developed sensor for detecting brain tumors with multiple graphene metasurfaces of SRR and CSRR, (e) Steps involved in the nanosensor design, (f) Metamaterial biosensor schematic, and (g) Metamaterial biosensor schematic[36-42]

In 2009, Basudev Lahiri and colleagues developed asymmetric split-ring resonators (A-SRRs) for optical sensing of organic compounds, as illustrated in Fig.2(a)[36]. The team fabricated gold-film A-SRRs on a fused silica substrate via standard electron-beam lithography and measured their reflection spectra using Fourier transform infrared spectroscopy (FTIR). Adjusting the angular gap between the A-SRR arcs allowed for tuning of the resonant frequency and enhancement of the quality factor. Notably, A-SRRs exhibited significant sensitivity to organic materials like polymethyl methacrylate (PMMA), with a 30-nm

PMMA layer causing a resonance shift of 120 nm. In 2014, Singh et al. employed THz asymmetric split-ring (TASR) metamaterials, as shown in Fig.2 (b)[37]. The TASR's quadrupole resonance achieved a *Q*-factor value of up to 65, and the *Q*-factor of the Fano resonance reached 28, surpassing that of symmetric structures of equivalent size.

Through structural refinement of the basic SRR design, the research team achieved enhanced sensing sensitivity. In 2021, the research team led by Jiahao Yang engineered two tunable THz metamaterial sensors[38] (designated as TTM-1 and TTM-2) based on concentric SRRs, as shown in Fig.2(c), exhibiting single-resonance and dual-resonance characteristics, respectively. Through precise modulation of the distance between the SRRs and the substrate, tunability of resonance frequencies was achieved, demonstrating a maximum frequency tuning range of 0.432 THz. The TTM-1 configuration exhibited a sensitivity of 0.54 THz/RIU and the FOM of 50.69 when subjected to a refractive index (*n*) of 1.1. Meanwhile, the TTM-2 variant demonstrated enhanced performance with a sensitivity of 1.12 THz/RIU and FOM of 39.98. In 2023, Osamah Alsalman and colleagues developed a high-performance sensor based on a composite structure of SRRs and complementary split-ring resonators (CSRRs) integrated with a graphene metasurface, designed for the efficient detection of brain tumors. A schematic illustration of the design is presented in Fig.2(d)[39]. The proposed sensor exhibited an exceptional sensitivity of 153.85 GHz/RIU within the frequency range of 0.25 THz to 0.45 THz, accompanied by the FOM of 3.98 and a *Q*-factor value of 8.54. Notably, at a chemical potential of 0.9 eV, the transmission spectrum reaches its minimum value of 0.579 at 0.316 1 THz, corresponding to the peak sensitivity of the device. In 2025, Bhagwati Sharan and colleagues proposed a novel THz metamaterial nanosensor based on SRR architecture for highly sensitive detection of cardiac biomarker NT-proBNP[40], as illustrated in Fig.2(e). The proposed sensor exhibited remarkable performance metrics, achieving an exceptional sensitivity of 1 460 GHZ/RIU. Furthermore, the device demonstrated superior resonance characteristics with a *Q*-factor of 22.06 and the outstanding FOM reaching 41.71, indicating its potential for precise cardiac biomarker detection applications.

The emergence of multi-SRRs resonant unit structures also provides a solution for improving sensitivity. In 2021, a microstructured biosensor composed of cut lines and SRRs[41] was proposed to achieve polarization-independent electromagnetically induced transparency (EIT) at THz frequencies, as shown in Fig.2(f). When the characteristics of the analyte change, the EIT-like resonance experiences simultaneous changes in resonance frequency and amplitude. The sensitivity of this biosensor is as high as 496.01 GHz/RIU. The research team led by Yungui Xiao developed an innovative tunable THz metamaterial sensor utilizing SRR architecture, which achieves active modulation of multiple resonance characteristics through dynamic geometric parameter control[42], as shown in Fig.2(g), The sensor demonstrated remarkable performance metrics, attaining 74% transmission intensity modulation at 0.856 THz. Furthermore, it exhibited superior resonance properties with *Q*-factor values of 18.4 at 0.734 THz and 21.4 at 0.856 THz, representing significant advancements in THz sensing technology.

Meanwhile, THz sensors featuring three-dimensional SRR structures have been increasingly developed[43]. These structures enhance the electromagnetic field's spatial dimensionality, thereby improving sensitivity by expanding the contact area with the target substance. In 2016, Wu et al. introduced a metamaterial sensor comprising four U-shaped SRRs[44], depicted in Fig.3(a). This sensor achieved a sensitivity of 470.6 nm/RIU and the FOM value of 250. In the same year, Yongzhi Cheng's team designed a novel all-metal plasmonic perfect absorber (PA) featuring four-forked rod resonators (FRRs) [45], depicted in Fig.3(b). The absorption peak of this structure can be tuned by altering the geometric parameters of the FRRs. This PA demonstrates high sensitivity to changes in the surrounding mediums' refractive index, achieving 1 445 nm/RIU and the FOM of 28.8. In 2017, Wei Wang and colleagues developed a THz sensor with a double-open vertical structure[46], illustrated in Fig.3(c). This double-split SRR sensor exhibits a sensitivity of 788 GHz/RIU, a *Q*-factor value of approximately 20, and the FOM of around 10. In 2018, Siyu Tan and co-authors introduced an ultrasensitive THz absorption sensor based on a three-dimensional SRR[47], shown in Fig.3(d). It boasts the FOM of 60.09 and a maximum refractive index sensitivity of 34.40% RIU. This sensor maintains high sensitivity under transverse magnetic (TM)-polarized incidence up to 60°and shows a high tolerance for structural deviations.

In summary, since a large amount of charges can accumulate at the opening of the SRR structural unit, forming a strong electromagnetic field, and the *Q*-factor value of the resonant frequency is usually high, this structure is widely used in sensing. SRR and its variant structures have become a classic category in the design of THz sensors.

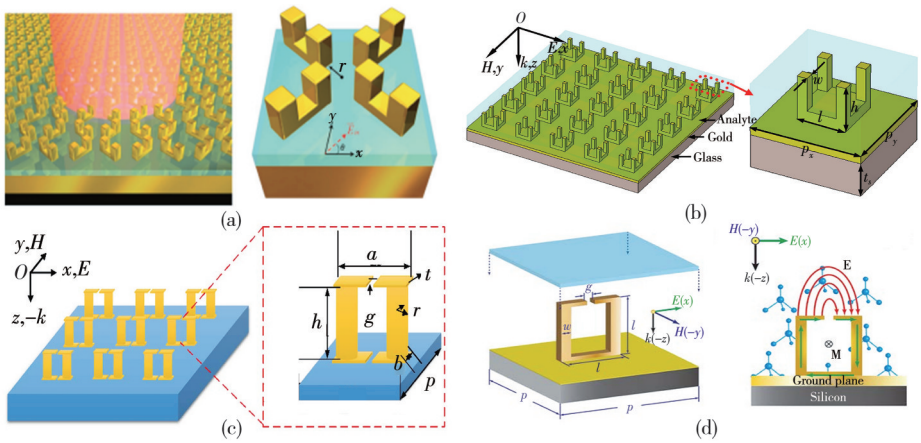

Fig. 3 Three-dimensional SRR structure sensors. (a) Schematic of an isotropic perfect absorber utilizing four-VSRRs; (b) Three-dimensional array and unit cell configuration of the plasmonic PA, (c) Schematic of the unit cell structure featuring a double-open vertical SRR, (d) Left panel illustrates the unit cell of an ultra-sensitive terahertz absorption sensor based on a three-dimensional split-ring resonator, while right panel depicts the electric and magnetic fields within the sensor, with the molecule at the top symbolizing the analyte[44-47]

2.2 Characteristic absorption peak sensors based on photonic crystal microstructures

Photonic crystals are periodic dielectric structures possessing a photonic band gap (PBG), which enables the control of photon propagation. When external environmental factors (e.g., temperature, pH, mechanical stress) alter the lattice parameters or the refractive index of the photonic crystal, the associated PBG shifts, consequently leading to a change in its structural color [48]. Their distinctive BPGs and customizable optical properties make them valuable for detecting heat, force, magnetism, chemicals, and biomolecules. Consequently, they have been integrated into mainstream sensing systems, including physical, chemical, and biosensors. Photonic crystals can serve as an enhancing substrate for SPR sensors, amplifying the electromagnetic field through the photonic localization effect. They can also be integrated with waveguide structures to form photonic crystal waveguides, thereby improving the light confinement ability.

Okamoto et al. fabricated a photonic crystal cavity THz sensing system[49]. As depicted in Fig. 4(a), this system implemented a photonic crystal (PC) resonator configuration in conjunction with a miniaturized resonant tunneling diode (RTD) that performed both excitation and sensing functions. The refractive index sensing functionality was systematically evaluated by depositing dielectric layers with precisely controlled thickness gradients onto the photonic crystal cavity, followed by high-precision measurement of the induced resonant index variations. Fig. 4(b) shows the experimental resonance spectra for different strip thicknesses, where an increase in strip thickness leds to a red-shift in the resonance frequency peak. The experimental data, as presented in Fig. 4(c), align well with the simulated curve. By tuning the DC voltage of the thermistor, the frequency of the thermistor-based signal source could be swept from 0.316 THz to 0.321 THz, enabling a compact, frequency-tunable signal source. The sensor achieves a Q-factor value exceeding 1×10^4 at the resonance frequency of 318 GHz. In 2017 work, Xiaomei Shi and colleagues engineered a one-dimensional photonic resonant cavity specifically configured for α-lactose detection applications. As shown in Fig.4(d), this system adopts a 1D photonic crystal defect mode architecture comprising two mirror-symmetric Bragg reflectors enclosing a central defect region. As shown in Fig. 4(e), the resonant transmittance of this structure is close to 100%. As shown in Fig.4(f), the introduction of alternative analytes exhibiting distinct absorption characteristics to the sensor interface induces a measurable red shift in the resonance frequency, thereby confirming the system's specific detection capability[50]. In 2019, the study by Wei Cheng and co-workers reported a high-performance sensor system built upon a photonic crystal cavity configuration, which can specifically and sensitively recognize lactose and fructose. As shown in Fig. 4(g), it consists of two identical photonic crystal plates, and each photonic crystal plate is composed of a square lattice of silicon-based cylindrical pillars. As shown in Fig.4(h), the pillars are located on the silicon substrate. Upon lactose deposition on the sensor interface, the resonant peak amplitude exhibits a progressive attenuation with increasing lactose film thickness, demonstrating a remarkable sensitivity enhancement of 31-fold compared to the bare substrate. As shown in Fig.4(i), fructose interaction with the sensor interface induces a significant positional shift of

the resonance peak. This proves the ability of the sensor to distinguish different samples[51].

In summary, the THz sensor designed based on the photonic crystal cavity structure cannot only achieve a high Q-factor value (up to the order of thousands to hundreds of thousands), but also shows great potential application value in the field of biomolecule recognition and detection, laying a theoretical and technical foundation for its in-depth development in the direction of biosensing.

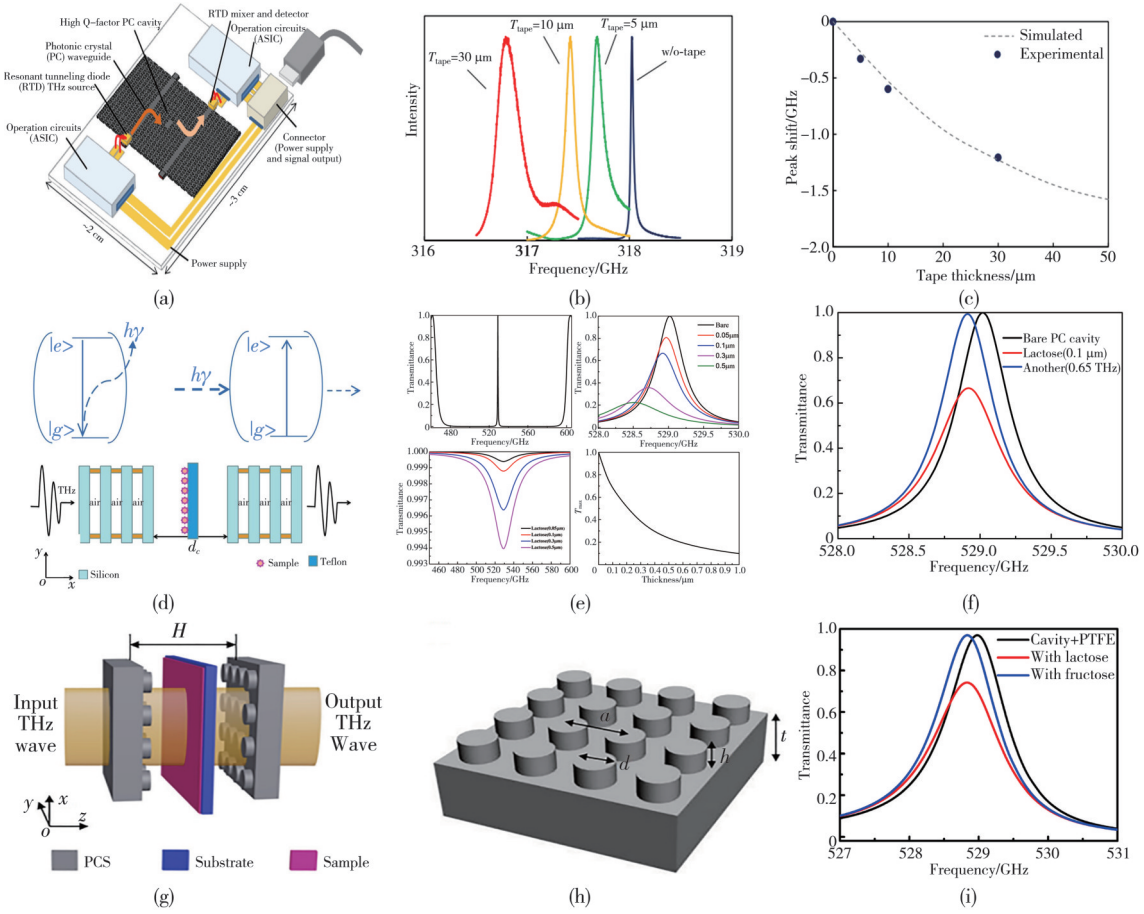

Fig. 4 THz sensors based on photonic crystal microstructures. (a) Composite sensing unit integrating a photonic crystal cavity and a resonant tunneling diode, (b) Spectral response profiles for thickness gradient detection of polyester tape samples, (c) Variation of resonance frequency peak with tape thickness, (d) Diagrammatic representation of a one-dimensional photonic bandgap structure featuring a defective cavity region, (e) Evolution of the transmission spectrum in the photonic crystal structure, (f) Impact of lactose specimens and reference materials on the transmission spectral profile, (g) Structural diagram illustrating photonic crystal defect cavity system, (h) Schematic diagram of PCS structure, and (i) Evaluation of resonant peak modulation by fructose versus lactose samples[49-51]

2.3 THz sensors with characteristic absorption peaks based on waveguide resonator structures

Waveguide structures confine electromagnetic waves along the transmission axis, facilitating their transfer with minimal magnetic field loss[52]. A waveguide resonator confines light within micro- or nano-scale channels through total internal reflection, establishing resonant modes. A change in the refractive index within the sensing region induces a shift in the resonant frequency, and detection is achieved by monitoring this spectral shift of the resonance peak. This low-loss structural design facilitates the realization of ultrahigh sensitivity. Its inherent compatibility with lab-on-a-chip platforms allows for multiplexed parameter analysis.

In 2009, Mendis et al. developed a parallel-plate waveguide (PPWG) resonator utilizing the lowest-order transverse electric (TE1) mode[53], depicted in Fig.5(a). This resonator, used to detect resonant frequency shifts in various N-alkane samples, demonstrated a refractive index sensitivity of 3.7×10^5 nm/RIU in the THz range. In 2011, Reichel et al. created a THz multi-channel microfluidic sensor based on PPWG geometry[54], illustrated in Fig.5(b). The groove width and spacing were optimized using the finite element method to ensure distinct resonances per groove. Experimentally, resonances at 265 GHz and 290 GHz were achieved, with high Q-factors values of 32 and 88, respectively.

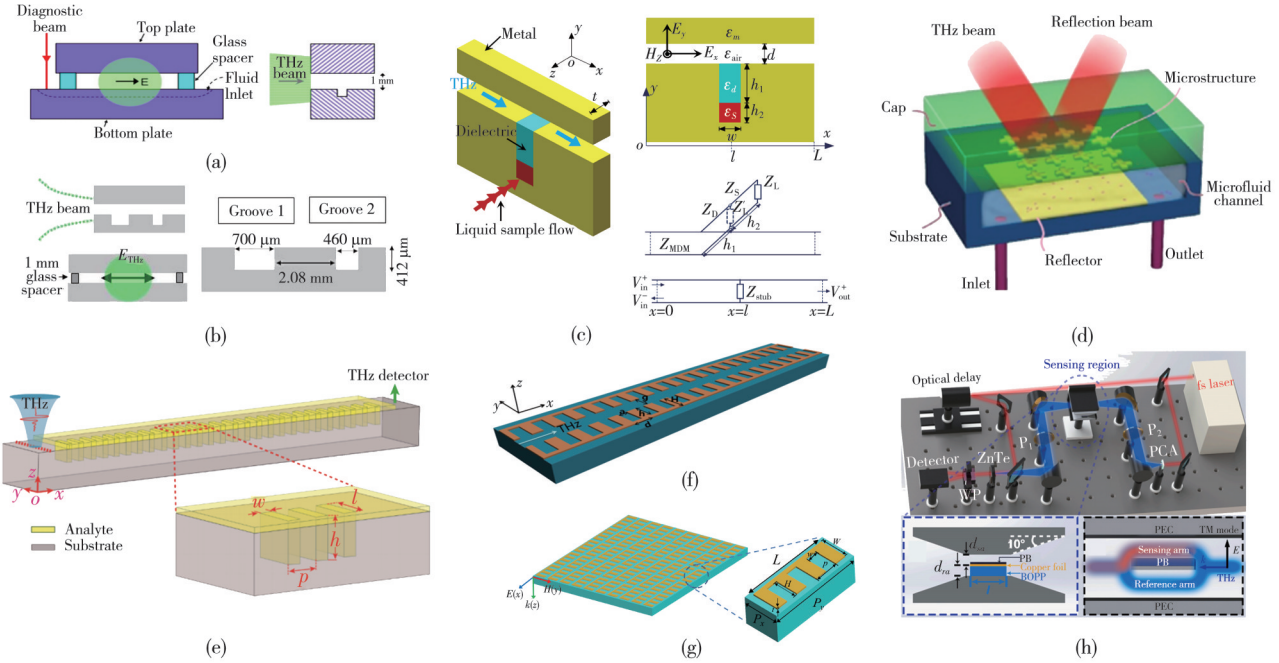

Fig. 5 THz sensors based on waveguide resonator structures. (a) Parallel-plate waveguide (PPWG) resonator, (b) Schematic of PPWG sensor and experimental setup, illustrating waveguide and groove geometry, and waveguide's orientation to incident terahertz beam, (c) THz sensor utilizing metal-dielectric-metal (MDM) waveguide structure, (d) Schematic of microfluidic (MAIM) sensor, (e) Planar surface plasmon waveguide terahertz sensor, (f) THz sensor with a comb-shaped metal waveguide structure, (g) THz sensor featuring a planar comb-shaped antenna array, and (h) THz Mach-Zehnder interferometer (MZI) sensor[53-60]

In 2015, Li et al. designed a THz metal-dielectric-metal (MDM) waveguide sensor[55], which was used to detect the change in the refractive index of liquids trough an embedded microfluidic channel, as shown in Fig. 5(c). This sensor achieved a refractive index sensitivity of up to 0.457 THz/RIU in a cross-sectional channel of 20 μm × 24 μm. Hu et al. integrated a microfluidic channel into an MDM structure. This novel sensor achieved a significantly enhanced light-matter interaction in the THz frequency band[56], as shown in Fig.5(d). This sensor had high sensitivity when operating near 1 THz, reaching 3.5 THz/RIU. In 2017, Islam et al. designed a planar surface plasmon waveguide THz sensor[57], as shown in Fig.5(e), and studied the dispersion relation of a rectangular groove waveguide filled with polyimide at different refractive indices. As the sample volume increased, the sensitivity and FOM of the waveguide also increased. For a sample of 0.025 mm^3, the sensitivity and FOM were 0.06 THz/RIU and 8.74, respectively.

Metallic waveguides, traditionally utilized in the microwave frequency range, can be adapted for the THz range by reducing their dimensions. In 2017, Shi et al. designed a comb-structured metallic waveguide specifically for lactose sensing applications, as illustrated in Fig. 5(f) [58]. This waveguide features two opposing metallic strips and a unilateral comb-shaped corrugation. It effectively detects thin-layer lactose, demonstrating sensitivity to thicknesses of only a few micrometers. The waveguide's transmission spectrum exhibits a pronounced dip at the characteristic absorption frequency of 0.529 THz, a feature absent in the transmission through a lactose layer of equivalent thickness. Fei Shen and colleagues demonstrated ultrasensitive lactose detection in 2019 through the implementation of a planar comb-structured antenna array configuration[59], as shown in Fig. 5(g). The incorporation of the antenna array within the device architecture significantly improves the THz radiation-lactose interaction efficiency. Compared with using a silicon substrate, the sensing signals in the transmission and reflection modes for lactose sensing using the antenna array are increased by 7.6 times and 13 times, respectively. In a 2024 study, an innovative THz Mach-Zehnder interferometer (MZI) sensor was constructed using a dual-channel PPWG for the detection of reducing drugs on a chip, as shown in Fig. 5(h). This sensor realizes selective detection of cysteamine by in-situ growing Prussian blue (PB) inside the sensing arm. The detection sensitivity of this sensor for cysteamine reaches 0.09 GHz/nmol, the detection limit is 88 nmol, and the maximum response difference is 4.2 times compared with other configurations, verifying its high sensitivity and selectivity[60]. In summary, the advantage of waveguide sensors lies in their wide operating frequency range, which enables effective detection of a broader range of samples.

2.4 THz sensors with spoof surface plasmon resonance (spoof SPR) structures

When the external light field couples with the metal-dielectric heterogeneous interface, the free carriers inside the metal will exhibit a cooperative oscillation behavior, which in turn excites surface waves propagating along the metal-dielectric interface. This phenomenon is known as surface plasmon resonance[61]. By constructing periodic slit and hole arrays on the metal surface, the propagation of surface plasmon waves can be effectively simulated, and the interaction between electromagnetic waves and the metal surface can be enhanced, thereby achieving highly sensitive sensing detection[62]. This surface plasmon resonance technology realized by artificial microstructures is called spoof surface plasmon resonance (Spoof SPR). This structured sensor enables label-free detection, eliminating the need for fluorescent or radioactive labels and thereby preserving the native activity of biomolecules. It also facilitates real-time dynamic monitoring, allowing for the continuous tracking of molecular binding and dissociation kinetics, which makes it highly suitable for the analysis of low-concentration biomarkers. SPR technology serves as a cornerstone of optical sensing, and its electromagnetic field enhancement mechanism provides a theoretical basis for other sensors.

In 2004, Pendry et al. successfully achieved Spoof SPR[63] by creating periodic slits and hole arrays on the metal surface, as shown in Fig. 6(a). Research indicates that holes can mimic real surface plasmons. By drilling holes in the metal surface, surface plasmons can be induced at almost any frequency, thereby controlling and guiding radiation, which provides the possibility for designing novel optical devices. In 2020, the study by Wei Cheng and co-workers reported a precisely fabricated resonant nano-slot structure with tailored optical properties, as shown in Fig. 6(b) [64]. This structural configuration enabled the discrimination of characteristic fingerprint spectra from diverse sugar molecules (including lactose and maltose) while maintaining invariant geometric parameters. Applying lactose to the slit resulted in a transmission valley at a specific frequency on the transmission curve. Conversely, when maltose was adhered, the transmission valley shifted to a different frequency. This indicates that the structure can perform precise fingerprint recognition for different sugars.

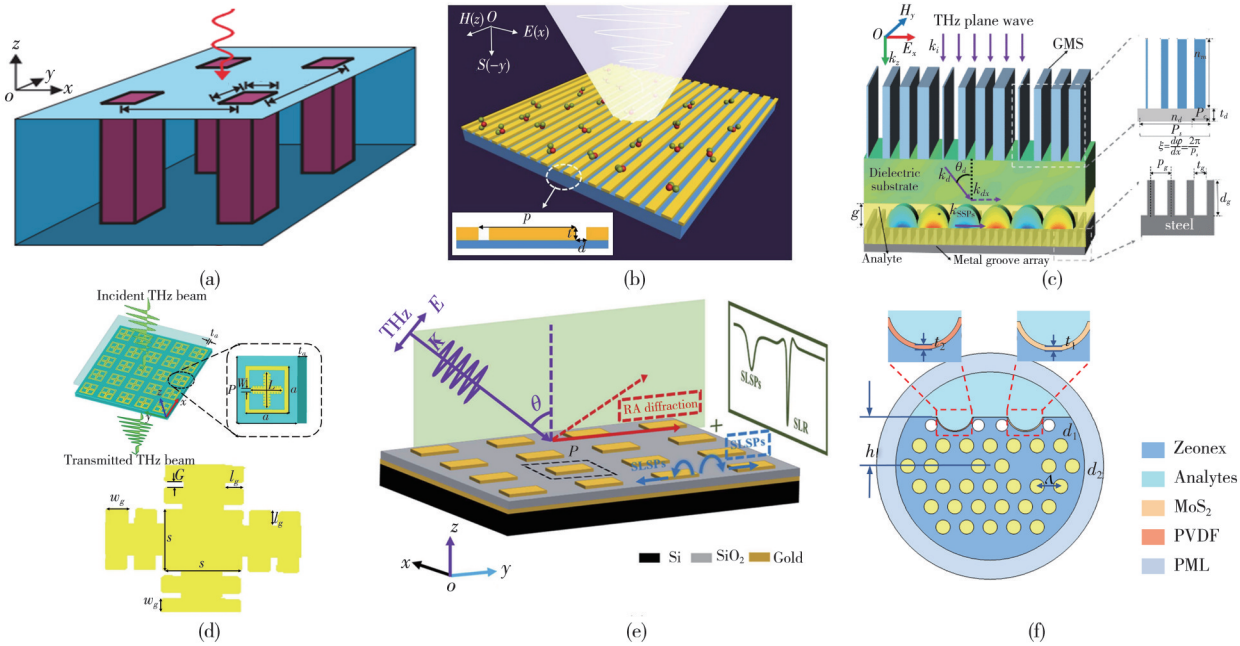

Fig. 6 Terahertz sensors with spoof surface plasmon resonance structures. (a) Schematic of a periodically structured ideal conductor metal groove, (b) Resonant nanoslot structure, (c) Architecture of the 1D dielectric GMS-coupled terahertz SSP sensing platform, (d) A schematic of designed THz metasensor covered by an analyte layer, (e) SLR metasurface array architecture for SLR generation, and (f) Cross section of designed SPR-MSF sensor[63-68]

In 2022, the research team led by Dexian Yan proposed an innovative design for THz spoof surface plasmon polariton (SSPPs) sensors based on all-dielectric gradient metasurface (GMS) couplers[65], as shown in Fig. 6(c). Operating at 0.46 THz, the sensor demonstrated exceptional performance characteristics, exhibiting an ultrahigh sensitivity of 517.9 GHz/RIU to refractive index variations in gap media while maintaining a Q-factor value of 262. Remarkably, the sensor retained a substantial sensitivity of 410 GHz/RIU even when detecting larger refractive index changes. The research team led by Ruchi Bhati developed a novel THz metamaterial sensor based on

SSPPs[66], featuring a hybrid architecture combining square split-ring resonators with cross-shaped groove resonators within a 68 μm periodic unit cell for dual-band high-sensitivity detection, as shown in Fig.6(d). In 2024, the research team led by Hongshun Sun proposed a highly sensitive biochemical sensor based on surface lattice resonance (SLR) metasurfaces[67], as demonstrated in Fig.6(e). The device achieved an unprecedented quality factor of 164.4 coupled with a refractive index sensitivity reaching 502.8 GHz/RIU. Experimental evaluation using physiological 0.9% NaCl solution (0.153 8 mol/L) revealed a measurable frequency shift of 246.8 GHz, substantiating the sensor's exceptional detection capability. In 2025, Pinna Wang's research team developed an innovative SPR biosensor based on dual-microgroove dual-core microstructure fiber (MSF) for THz applications[68], as shown in Fig. 6(f). The sensor incorporated a novel design featuring molybdenum disulfide (MoS_2) and polyvinylidene fluoride (PVDF) coatings on polished side surfaces, enabling dual independently tunable SPR resonance peaks. Operating within the analyte refractive index range of 1.30 to 1.39, the sensor demonstrated outstanding performance metrics. The primary resonance peak achieved maximum wavelength and amplitude sensitivities of 467.2 μm/RIU and 101.202/RIU respectively, while the secondary peak reached 625.3 μm/RIU and 113.927/RIU. Corresponding FOMs were measured at 65.987/RIU for the primary peak and 67.037/RIU for the secondary peak, with minimum detectable refractive index changes of 2.14×10^{-7} RIU and 1.6×10^{-7} RIU, respectively. Operating within the analyte refractive index range of 1.30 to 1.39, the sensor demonstrated outstanding performance metrics. The primary resonance peak achieved maximum wavelength and amplitude sensitivities of 467.2 μm/RIU and 101.202/RIU respectively, while the secondary peak reached 625.3 μm/RIU and 113.927/RIU. Corresponding FOMs were measured at 65.987/RIU for the primary peak and 67.037/RIU for the secondary peak, with minimum detectable refractive index changes of 2.14×10^{-7} RIU and 1.6×10^{-7} RIU, respectively.In summary, the Spoof SPR structure can perform refractive index sensing by observing phase information, which is superior to traditional amplitude measurement.

2.5 THz sensors based on integrated deep learning

Metasurface designs employing multiplexing schemes demonstrate significant potential for enhancing trace detection of molecular fingerprints in the THz regime. Conventional approaches rely on matching spectral resonance positions with molecular fingerprints of trace analytes, necessitating laborious metastructure optimization through extensive optical simulations. Recent advances have revealed the considerable promise of deep learning techniques in revolutionizing metasurface design methodologies[69-70]. Deep learning establishes correlations between metastructures and optical responses through artificial neural networks, effectively bypassing the need to solve Maxwell's equations directly. This approach demonstrates remarkable advantages over conventional numerical methods by substantially reducing computational costs in simulations[71-72].

In 2025, the research team led by Jingxiao Yu developed a novel metamaterial sensor featuring a circle-cross composite structure comprising a polyimide dielectric layer and gold resonant layer[73], as depicted in Fig.7(a). Through deep learning optimization, the team achieved optimal structural parameters including substrate thickness (18 μm), metal thickness (0.2 μm), ring width (6 μm), cross length (61 μm), and cross width (1.8 μm). The optimized sensor demonstrated dual resonant peaks at 0.806 6 THz and 1.643 6 THz, with an average Q-factor value of 2.323 2. The device exhibits exceptional sensitivity metrics of 0.050 87 THz/μm for thickness measurement.

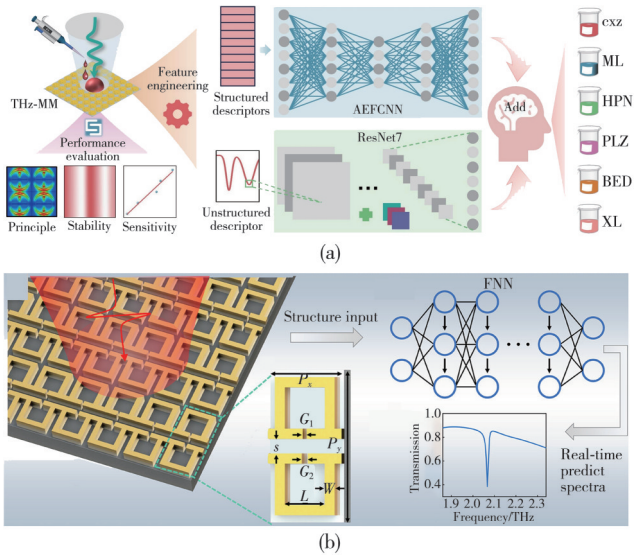

Fig. 7 THz sensors based on integrated deep learning. (a) Schematic illustration of the dual-band THz metamaterial sensor integrated with a deep learning model fusing one-dimensional and two-dimensional descriptors for synergistic identification of red wine varieties, and (b) Multiparameter-optimized metasurface biosensor design[73]

The research team led by Shengfeng Wang developed a transfer learning-enabled multi-objective optimization methodology for THz quasi-bound state in continuum (QBIC) metasurface biosensors[74], as depicted in Fig.7(b). The study introduced an innovative two-stage transfer

learning paradigm, commencing with pre-training on 131 low-dimensional samples followed by knowledge transfer to 17 161 high-dimensional parameter configurations. This approach achieved exceptional performance metrics, including a Q-factor value of 839.56 and FOM of 158.91, while demonstrating 36 000-fold computational acceleration and 50% reduction in data requirements. The research employed a tandem neural network architecture integrated with random forest algorithms, enabling the first quantitative assessment of individual performance indicator contributions.

Table 1 summarizes the THz sensor parameters (sensitivity S, quality factor Q, and FOM) under different microstructures. The comparative performance differences among various microstructures are presented for direct analysis. The THz sensor based on the SRR structure primarily exhibits advantages of mature fabrication processes, multi-parameter detection capability, and ease of integration, yet its limitations lie in sensitivity to substrate losses and stringent requirements for fabrication precision. Such sensors are well-suited for scenarios requiring the simultaneous detection of multiple indicators, such as the rapid preliminary screening for various toxins and contaminants in food safety, as well as for diverse gaseous or liquid pollutants in environmental monitoring. Photonic crystal-based THz sensors are characterized by their exceptionally high quality factor (Q) and ultrahigh resolution, though they face challenges in complex fabrication procedures and defect structure design.

Table 1 Image performance results

Microstructure	S/(GHz•RIU^{-1})	Q	FOM	Ref.
SRR	540	84.70	50.69	[38]
	153.85	8.54	3.98	[39]
	1 460	26.0	41.71	[40]
	496.01	—	—	[41]
	—	48.7	—	[42]
Photonic crystal microstructures	—	10,800	—	[2]
	—	1 150	—	[50]
	—	529	—	[51]
Waveguide resonator structures	225	32	7.03	[53]
	457	—	3.1	[55]
	3 500	—	—	[56]
	130	—	16.75	[57]
	—	21	8.73	[58]
	750	—	—	[59]
Spoof SPR	517.9	262	—	[65]
	502.8	164.4	31.4	[67]
	113.927	—	67.03	[68]
Integrated deep learning	—	839.562 3	158.911 3	[74]

By being engineered to incorporate specific defect states, such sensors enable target-specific detection of biomarkers with ultrahigh sensitivity. This capability makes them exceptionally well-suited for the accurate validation of predetermined biomarkers in clinical diagnostics. Waveguide resonant cavity (WRC)-structured THz sensors demonstrate strengths in strong field localization, controllable mode profiles, and suitability for chip-level integration, but are constrained by risks of multi-mode interference and high demands on dimensional machining accuracy. The exceptional adaptability of this sensor for on-chip integration establishes it as a fundamental building block for lab-on-a-chip devices. It facilitates the monolithic integration of the complete workflow from sample preparation to data acquisition on a single substrate, offering a significant advantage in spatially confined environments. Spoof SPR-structured THz sensors achieve unparalleled sensitivity and theoretical FOM limits, albeit with significant drawbacks including substantial metallic losses, rigorous excitation conditions, and pronounced dependence on incident angle/polarization. This category of sensors is primarily employed in frontier scientific research to explore the theoretical limits of sensing, or to detect an extremely small number of molecules under extreme conditions, such as ultra-high vacuum.

Conventional THz sensors relying on artificially designed microstructures (e. g., SRRs, photonic crystals) and empirical signal analysis methods encounter critical limitations in complex sample detection scenarios, including sensitivity bottlenecks, difficulties in feature extraction, and inadequate generalization capabilities. Deep learning technology, through the construction of multi-layer neural network models, enables automated extraction of high-dimensional nonlinear mappings between THz signals (e. g., resonance frequency shifts, transmission spectra) and target material properties (e. g., refractive index, concentration, molecular configuration). This approach facilitates the attainment of superior Q-factor values and FOMs, thereby substantially enhancing the sensor's intelligence level and detection performance.

3 Conclusions

THz micro-structured sensing systems principally serve for material identification and quantitative detection based on analyte refractive indices, characteristic spectral patterns, or biological attributes. This review thoroughly examines various THz micro-structured sensors, emphasizing their structural features and foundational principles. These sensors demonstrate high sensitivity in analyte detection and possess the capability to specifically recognize different substances, making them highly promising in fields such as biomedicine, non-destructive testing, and food and agriculture[75]. Within the biomedical field, such systems facilitate the precise identification of

pathologically relevant molecular markers and disease-indicative substances, showing considerable promise for pre-symptomatic disease detection and therapeutic monitoring. In non-destructive evaluation, these techniques enable comprehensive material property characterization and manufacturing quality control across pharmaceutical and industrial production sectors. Throughout the global food and agriculture industry, they facilitate food quality control, pollutant detection, and freshness evaluation. The broad applicability and transformative potential of THz microstructured sensing platforms establish them as an emerging technology with considerable scientific and industrial value across multiple sectors.

The extraordinary sensitivity of THz micro-structured sensing platforms to refractive index perturbations allows for dramatic resonance peak displacement in response to minimal analyte refractive index changes, facilitating ultrasensitive quantitative analysis in uncomplicated system architectures[76]. Nevertheless, these sensors demonstrate constrained capability in differentiating and characterizing diverse substances within complex matrices[77-78], such as low sensitivity when detecting micron - and nano - thin film materials[79], and the MDM waveguide sensing platform in the THz band remains rarely explored[80]. In parallel, THz-based fingerprinting sensors utilize the intrinsic absorption characteristics of biological molecules to accomplish selective substance recognition. Although they are specific, currently, fingerprint sensors have low sensitivity and poor detection accuracy. Ongoing research efforts have focused on investigating diverse sensor architectures to enhance both sensitivity performance and measurement precision[81-83]. Biosensing platforms exploit the distinctive molecular recognition capabilities of biomolecules-including highly specific binding affinities-to overcome the inherent sensitivity and accuracy constraints of conventional fingerprint sensors. These advanced biosensors have demonstrated remarkable efficacy in detecting malignant neoplastic cells[84-85], neoplastic cellular populations[86], pathogenic bacterial strains[87], and enabling precise microscale liquid analysis[88].

Traditional metasurface design methods typically rely on complex electromagnetic simulations and finite element approaches, which employ extensive parameter scanning to identify optimal solutions, resulting in high computational costs and prolonged design cycles. With the rapid advancement of machine learning, deep learning-based design methods have been proposed to predict the mapping relationships between sensor structures and spectral responses, significantly improving design efficiency. Integrating deep learning with physical principles in metasurface design is also recognized as an effective strategy to enhance model performance. Looking forward, combining deep learning models with THz sensor design holds promise for achieving more efficient and sensitive detection and sensing capabilities.

Acknowledgement

This work was supported by National Natural Science Foundation of China (Nos. 62301509, 62405293), and General Project of China Postdoctoral Science Foundation (No.2025M770537).

Declaration of conflicting interests

The authors have no conflict of interests related to this publication.

References

[1] GORSHUNOV B, VOLKOV A, SPEKTOR I, et al. Terahertz BWO-spectrosopy. International Journal of Infrared and Millimeter Waves, 2005, 26(9): 1217-1240.

[2] OKAMOTO K, TSURUDA K, DIEBOLD S, et al. Terahertz sensor using photonic crystal cavity and resonant tunneling diodes. Journal of Infrared, Millimeter, and Terahertz Waves, 2017, 38(9): 1085-1097.

[3] YANG D, MEI H, YAO L, et al. 3D/4D printed tunable electrical metamaterials with more sophisticated structures. Journal of Materials Chemistry C, 2021, 9(36): 12010-12036.

[4] ROH Y, KIM T, LEE G, et al. Advances in terahertz biosensors toward photon-molecule interplay. TrAC Trends in Analytical Chemistry, 2024, 175: 117715.

[5] ZHAN X Y, LIU Y, CHEN Z G, et al. Revolutionary approaches for cancer diagnosis by terahertz-based spectroscopy and imaging. Talanta, 2023, 259: 124483.

[6] GEZIMATI M, SINGH G. Advances in terahertz technology for cancer detection applications. Optical and Quantum Electronics, 2022, 55(2): 151.

[7] SINGH K, AALAM U, MISHRA A, et al. Spectroscopic and imaging considerations of THz-TDS and ULF-Raman techniques towards practical security applications. Optics Express, 2024, 32(2): 1314-1324.

[8] CHENG Y Y, QIAO L B, ZHU D, et al. Passive polarimetric imaging of millimeter and terahertz waves for personnel security screening. Optics Letters, 2021, 46(6): 1233.

[9] WANG R D, XU L, WANG J Y, et al. Electric Fano resonance-based terahertz metasensors. Nanoscale, 2021, 13(44): 18467-18472.

[10] PODDAR H, JU S H, SHAKYA D, et al. A tutorial on NYUSIM: sub-terahertz and millimeter-wave channel simulator for 5G, 6G, and beyond. IEEE Communications Surveys & Tutorials, 2024, 26(2): 824-857.

[11] YOU X H, HUANG Y M, LIU S H, et al. Toward 6G μ

extreme connectivity: architecture, key technologies and experiments. IEEE Wireless Communications, 2023, 30(3): 86-95.

[12] CHACCOUR C, SOORKI M N, SAAD W, et al. Seven defining features of terahertz (THz) wireless systems: a fellowship of communication and sensing. IEEE Communications Surveys & Tutorials, 2022, 24(2): 967-993.

[13] ZHAO X F, YANG C L, CHEN X, et al. Characteristic fingerprint spectrum of α-synuclein mutants on terahertz time-domain spectroscopy. Biophysical Journal, 2024, 123(10): 1264-1273.

[14] SUN L, ZHAO L, PENG R Y. Research progress in the effects of terahertz waves on biomacromolecules. Military Medical Research, 2021, 8: 28.

[15] WANG H, XIE L, ALBO A, et al. Selective detection enabled by terahertz spectroscopy and plasmonics: Principles and implementations. TrAC-Trends in Analytical Chemistry, 2024: 180.

[16] HLOSTA P, NITA M, POWALA D, et al. Terahertz radiation in non-destructive testing of composite pyrotechnic materials. Composite Structures, 2022: 279.

[17] SHI S, YUAN S, ZHOU J, et al. Terahertz technology and its applications in head and neck diseases. iScience, 2023, 26(7): 107060.

[18] ZHENG Z P, ZHENG Y, LUO Y, et al. A switchable terahertz device combining ultra-wideband absorption and ultra-wideband complete reflection. Physical Chemistry Chemical Physics, 2022, 24(4): 2527-2533.

[19] VAFAPOUR Z, DUTTA M, STROSCIO M A. Sensing, switching and modulating applications of a superconducting THz metamaterial. IEEE Sensors Journal, 2021, 21(13): 15187-15195.

[20] PITCHAPPA P, KUMAR A, SINGH R, et al. Terahertz MEMS metadevices. Journal of Micromechanics and Microengineering, 2021, 31(11): 113001.

[21] ZHENG C L, LI H, ZANG H P, et al. Terahertz polarization detection based on the mode analysis of longitudinally polarized vortices. Optics & Laser Technology, 2024, 170: 110210.

[22] YAN D X, CUI J, LI X J, et al. Enhancement of wide-band trace terahertz absorption spectroscopy based on microstructures: a review. Physical Chemistry Chemical Physics, 2023, 25(46): 31542-31553.

[23] CHEN C X, KAJ K, HUANG Y W, et al. Tunable toroidal response in a reconfigurable terahertz metamaterial. Advanced Optical Materials, 2021, 9(22): 2101215.

[24] LI X J, LIU H D, HOU X M, et al. Dynamic tunable meta-lens based on a single-layer metal microstructure. Photonics, 2022, 9(12): 917.

[25] DU J N, LI T, XU Z K, et al. Structure–activity relationship in microstructure design for electromagnetic wave absorption applications. Small Structures, 2023, 4(11): 2300152.

[26] ZHOU Y, SUN J H, LI Z Y, et al. Regulating integral alignment of magnetic MXene nanosheets in layered composites to achieve high-effective electromagnetic wave absorption. Composites Science and Technology, 2024, 256: 110746.

[27] RAMACHANDRAN T, FARUQUE M R I, AL-MUGREN K S. Low thermal SRR metamaterial design with multi-layered structured for terahertz frequency applications. Results in Engineering, 2024, 21: 101753.

[28] BASERI A, KESHAVARZ A, HATEF A. A type of arrangement for photonic crystal structures interacting with a Terahertz wave with omnidirectional and thermal effects. Journal of Applied Physics, 2020, 127(21): 214304.

[29] REICHEL K S, ASTLEY V, JONES J, et al. Terahertz multichannel microfluidic sensor based on parallel-plate waveguide resonant cavities//2011 International Conference on Infrared, Millimeter, and Terahertz Waves, October 2-7, 2011, Houston, TX, USA. New York: IEEE, 2011: 1-3.

[30] KATS M A, WOOLF D, BLANCHARD R, et al. Spoof plasmon analogue of metal-insulator-metal waveguides. Optics Express, 2011, 19(16): 14860-14870.

[31] AUPIAIS I, GRASSET R, DAINEKA D, et al. Chiral TeraHertz surface plasmonics. ACS Photonics, 2024: 4c01076.

[32] WU D W, CHEN H. An asymmetric split ring resonator for refractive-based-sensor applications at terahertz frequencies. Microwave and Optical Technology Letters, 2015, 57(5): 1132-1135.

[33] ZHANG D P, LI Z, JIA B W, et al. Application of circuit analog optimization method in fast optimization of dynamically tunable terahertz metamaterial sensor. Physica Scripta, 2023, 98(6): 065502.

[34] WANG Z L, WANG X, WANG J L. Research advance on the sensing characteristics of refractive index sensors based on electromagnetic metamaterials. Advances in Condensed Matter Physics, 2021, 2021(1): 2301222.

[35] LI Y Y, CHEN X Y, HU F R, et al. Four resonators based high sensitive terahertz metamaterial biosensor used for measuring concentration of protein. Journal of Physics D: Applied Physics, 2019, 52(9): 095105.

[36] LAHIRI B, KHOKHAR A Z, DE LA RUE R M, et al. Asymmetric split ring resonators for optical sensing of organic materials. Optics Express, 2009, 17(2): 1107-1115.

[37] SINGH R, CAO W, AL-NAIB I, et al. Ultrasensitive terahertz sensing with high-Q Fano resonances in metasurfaces. Applied Physics Letters, 2014, 105(17): 171101.

[38] YANG J H, LIN Y S. Design of tunable terahertz metamaterial sensor with single- and dual-resonance characteristic. Nanomaterials, 2021, 11(9): 2212.

[39] ALSALMAN O, WEKALAO J, ARUN KUMAR U, et al. Design of split ring resonator graphene metasurface sensor for efficient detection of brain tumor. Plasmonics, 2024, 19(1): 523-532.

[40] SHARAN B, ELAYAN H, GHOSH A, et al. A terahertz split ring resonator nanosensor for cardiac biomarker detection. IEEE Sensors Journal, 2025, 25(18): 35394-35406.

[41] ZHANG J, MU N, LIU L H, et al. Highly sensitive detection

of malignant glioma cells using metamaterial-inspired THz biosensor based on electromagnetically induced transparency. Biosensors & Bioelectronics, 2021, 185: 113241.
[42] XIAO Y G, LIN Y S. Tunable terahertz metamaterial with single to triple modulation resonance characteristics. Materials Science and Engineering: B, 2025, 315: 118128.
[43] WU P C, SUN G, CHEN W T, et al. Vertical split-ring resonator based nanoplasmonic sensor. Applied Physics Letters, 2014, 105(3): 033105.
[44] WU P C, LIAO C Y, CHEN J W, et al. Isotropic absorption and sensor of vertical split-ring resonator. Advanced Optical Materials, 2017, 5(2): 1600581.
[45] CHENG Y Z, MAO X S, WU C J, et al. Infrared non-planar plasmonic perfect absorber for enhanced sensitive refractive index sensing. Optical Materials, 2016, 53: 195-200.
[46] WANG W, YAN F P, TAN S Y, et al. Ultrasensitive terahertz metamaterial sensor based on vertical split ring resonators. Photonics Research, 2017, 5(6): 571.
[47] TAN S Y, YAN F P, WANG W, et al. Ultrasensitive sensing with three-dimensional terahertz metamaterial absorber. Journal of Optics, 2018, 20(5): 055101.
[48] PAN H G, CUI N, PAN F, et al. High-sensitivity surface plasmon resonance refractive index sensor with high resolution based on D-shaped photonic crystal fiber. Journal of Optics, 2024, 53(1): 468-474.
[49] OKAMOTO K, TSURUDA K, DIEBOLD S, et al. Terahertz sensor using photonic crystal cavity and resonant tunneling diodes. Journal of Infrared, Millimeter, and Terahertz Waves, 2017, 38(9): 1085-1097.
[50] SHI X M, HAN Z H. Enhanced terahertz fingerprint detection with ultrahigh sensitivity using the cavity defect modes. Scientific Reports, 2017, 7: 13147.
[51] CHENG W, HAN Z H, DU Y, et al. Highly sensitive terahertz fingerprint sensing with high-Q guided resonance in photonic crystal cavity. Optics Express, 2019, 27(11): 16071.
[52] HAN B J, HAN Z H, QIN J Y, et al. A sensitive and selective terahertz sensor for the fingerprint detection of lactose. Talanta, 2019, 192: 1-5.
[53] MENDIS R, ASTLEY V, LIU J B, et al. Terahertz microfluidic sensor based on a parallel-plate waveguide resonant cavity. Applied Physics Letters, 2009, 95(17): 171113.
[54] REICHEL K S, ASTLEY V, JONES J, et al. Terahertz multichannel microfluidic sensor based on parallel-plate waveguide resonant cavities//2011 International Conference on Infrared, Millimeter, and Terahertz Waves, October 2-7, 2011, Houston, TX, USA. New York: IEEE, 2011: 1-3.
[55] LI X J, SONG J, ZHANG J X J. Design of terahertz metal-dielectric-metal waveguide with microfluidic sensing stub. Optics Communications, 2016, 361: 130-137.
[56] HU X, XU G Q, WEN L, et al. Metamaterial absorber integrated microfluidic terahertz sensors. Laser & Photonics Reviews, 2016, 10(6): 962-969.
[57] ISLAM M, CHOWDHURY D R, AHMAD A, et al. Terahertz plasmonic waveguide based thin film sensor. Journal of Lightwave Technology, 2017, 35(23): 5215-5221.
[58] SHI X M, QIN J Y, HAN Z H. Enhanced terahertz sensing with a coupled comb-shaped spoof surface plasmon waveguide. Optics Express, 2017, 25(1): 278-283.
[59] SHEN F, QIN J Y, HAN Z H. Planar antenna array as a highly sensitive terahertz sensor. Applied Optics, 2019, 58(3): 540-544.
[60] MA L, FAN F, SHI W N, et al. Terahertz on-chip sensor based on Mach-Zehnder waveguide interferometer for selective recognition of reducing drug. Sensors and Actuators A: Physical, 2024, 370: 115282.
[61] MAIER S A, ANDREWS S R, MARTÍN-MORENO L, et al. Terahertz surface plasmon-polariton propagation and focusing on periodically corrugated metal wires. Physical Review Letters, 2006, 97(17): 176805.
[62] JOY S R, EREMENTCHOUK M, MAZUMDER P. Spoof surface plasmon resonant tunneling mode with high quality and Purcell factors. Physical Review B, 2017, 95(7): 075435.
[63] PENDRY J B, MARTÍN-MORENO L, GARCIA-VIDAL F J. Mimicking surface plasmons with structured surfaces. Science, 2004, 305(5685): 847-848.
[64] QIN J Y, CHENG W, HAN B J, et al. Ultrasensitive detection of saccharides using terahertz sensor based on metallic nano-slits. Scientific Reports, 2020, 10: 3712.
[65] YAN D X, LI X J, MA C, et al. Terahertz refractive index sensing based on gradient metasurface coupled confined spoof surface plasmon polaritons mode. IEEE Sensors Journal, 2022, 22(1): 324-329.
[66] BHATI R, JEWARIYA M, MALIK A K. Spoof surface plasmon-based terahertz metasensor for glucose and ethanol. Applied Physics A, 2022, 128(9): 840.
[67] SUN H S, CAO Y H, LI L Y, et al. A high-efficiency terahertz sensor based on surface lattice resonance metasurface for biochemical detection. Sensors and Actuators A: Physical, 2024, 377: 115711.
[68] WANG P N, ZHANG Y N, GUANG Z, et al. A dual-resonance peak biosensor based on surface plasmon resonance in the terahertz region. Physica Scripta, 2025, 100(10): 105524.
[69] CHEN W, GAO Y, LI Y Y, et al. Broadband solar metamaterial absorbers empowered by transformer-based deep learning. Advanced Science, 2023, 10(13): 2206718.
[70] XIONG J K, SHEN J Q, GAO Y, et al. Real-time on-demand design of circuit-analog plasmonic stack metamaterials by divide-and-conquer deep learning. Laser & Photonics Reviews, 2023, 17(3): 2100738.
[71] KHORAM E, WU Z C, QU Y R, et al. Graph neural networks for metasurface modeling. ACS Photonics, 2023, 10(4): 892-899.
[72] CHEN W, LI Y Y, LIU Y N, et al. All-dielectric SERS metasurface with strong coupling quasi-BIC energized by transformer-based deep learning. Advanced Optical Materials, 2024, 12(4): 2301697.
[73] YU J X, PU H B, SUN D W. Dual-band terahertz

metamaterial sensor integrated with deep learning for synergistic identification of red wine varieties. Chemical Engineering Journal, 2025, 520: 166006.

[74] WANG S F, LIU B W, WU X, et al. Transfer learning empowered multiple-indicator optimization design for terahertz quasi-bound state in the continuum biosensors. Advanced Science, 2025, 12(27): 2504855.

[75] SAADELDIN A S, HAMEED M F O, ELKARAMANY E M A, et al. Highly sensitive terahertz metamaterial sensor. IEEE Sensors Journal, 2019, 19(18): 7993-7999.

[76] CHEN X, FAN W H, JIANG X Q, et al. High-Q toroidal dipole metasurfaces driven by bound states in the continuum for ultrasensitive terahertz sensing. Journal of Lightwave Technology, 2022, 40(7): 2181-2190.

[77] HE Y H, TANG C, NIU Q S, et al. Dual resonance effects of electromagnetically induced transparency-like and Fano-like using terahertz metamaterial resonator. Optical and Quantum Electronics, 2020, 52(2): 58.

[78] LIU Y W, ZHENG D Y, CHEN P Y, et al. Tunable terahertz metamaterial using fractal microheater for refractive index sensing application. Journal of Materials Science, 2022, 57(48): 21935-21945.

[79] SINGH R, CAO W, AL-NAIB I, et al. Ultrasensitive terahertz sensing with high-*Q* Fano resonances in metasurfaces. Applied Physics Letters, 2014, 105(17): 171101.

[80] LI M P, SHI Y P, LIU X Y, et al. High-Q Fano resonance in subwavelength stub-wall-coupled MDM waveguide structure and its terahertz sensing application. IEEE Access, 2021, 9: 123939-123949.

[81] DENG X X, SHEN Y C, LIU B W, et al. Terahertz metamaterial sensor for sensitive detection of citrate salt solutions. Biosensors, 2022, 12(6): 408.

[82] SONG J M, SHI Y P, LI M P, et al. Enhanced extraordinary terahertz transmission through coupling between silicon resonators. Nanoscale Advances, 2022, 4(11): 2494-2500.

[83] SHALABY M, MERBOLD H, PECCIANTI M, et al. Concurrent field enhancement and high transmission of THz radiation in nanoslit arrays. Applied Physics Letters, 2011, 99(4): 041110.

[84] ZHANG C B, XUE T J, ZHANG J, et al. Terahertz toroidal metasurface biosensor for sensitive distinction of lung cancer cells. Nanophotonics, 2021, 11(1): 101-109.

[85] YANG K, YANG X, ZHAO X, et al. THz spectroscopy for a rapid and label-free cell viability assay in a microfluidic chip based on an optical clearing agent. Analytical Chemistry, 2019, 91(1): 785-791.

[86] ZHU M, ZHANG L, MA S Q, et al. Terahertz metamaterial designs for capturing and detecting circulating tumor cells. Materials Research Express, 2019, 6(4): 045805.

[87] SHI J, TIAN L L, SU M Y, et al. Surface bio-sensor based on terahertz Bragg fiber. Laser Physics, 2021, 31(10): 105102.

[88] ZHANG R, CHEN Q M, LIU K, et al. Terahertz microfluidic metamaterial biosensor for sensitive detection of small-volume liquid samples. IEEE Transactions on Terahertz Science and Technology, 2019, 9(2): 209-214.

基于微观结构的太赫兹传感技术：从电磁响应增强到多尺度检测

张　姝[1]，牛文宇[2]，郝亚峰[2]，马富鹏[2]，朱　璞[2]，武慧嘉[2]，黄育杰[2]，李腾腾[2*]，刘美宏[2*]，雷　程[2]，梁　庭[2]

1. 天津津航技术物理研究所，天津 300308；

2. 中北大学 极限环境光电动态测试技术与仪器全国重点实验室，山西 太原 030051

摘　要：太赫兹波具有高透射、强吸收和低光子能量等特性，在生物医学诊断、无损检测以及食品与农产品质量安全监测等领域具有广泛的应用，基于太赫兹波的传感器也因此受到越来越多的关注。然而，传统耦合结构设计与太赫兹波的高频振荡特性难以有效契合，导致信号能量传输效率低下，限制了太赫兹传感器的性能。而微结构技术通过构造亚波长共振单元与太赫兹波高频振荡特性的精确匹配，实现了电磁场能量的局域化增强，显著增强了太赫兹传感器灵敏度。本文总结了部分基于开口环谐振器、光子晶体、波导谐振腔与表面等离子体共振等不同微结构的太赫兹传感器基本原理及研究现状。尤其值得关注的是，近年来人工智能特别是深度学习技术发展迅速，其在信号处理、模式识别与逆向设计等领域的强大能力正逐步渗透至太赫兹传感技术领域。将深度学习算法与太赫兹传感器设计相结合，不仅能够有效挖掘复杂太赫兹信号中隐含的物质特征信息，提升目标识别与分类精度，还可通过对微结构参数空间的智能搜索与优化，辅助甚至自主完成高性能太赫兹传感结构的逆向设计与性能预测。这一跨学科融合趋势为突破传统设计方法的局限性、实现太赫兹传感器性能的跨越式提升开辟了新的路径。

关键词：太赫兹；人工微结构；传感器；表面等离子体共振；波导；光子晶体；深度学习

引用格式：ZHANG Shu, NIU Wenyu, HAO Yafeng, et al. Microstructure-based terahertz sensing technology: from electromagnetic response enhancement to multi-scale detection. Journal of Measurement Science and Instrumentation, 2026, 17(1): 1-15. DOI: 10.62756/jmsi.1674-8042.2026001